ISPRS Annals of the Photogrammetry, Remote Sensing and Spatial Information Sciences, Volume X-5/W4-2025
Philippine Geomatics Symposium (PhilGEOS) 2025 "Enhancing Human Quality of Life through Geospatial Technologies",
24–25 November 2025, Quezon City, Philippines

Optimized Surface Water Extraction for Planform Morphology Assessment of Pagsanjan-Lumban Watershed

Jayson L. Arizapa[1], Cristino L. Tiburan Jr.[1], Izuru Saizen[2]

[1]Institute of Renewable Natural Resources, College of Forestry and Natural Resources, University of the Philippines Los Baños
- jlarizapa1@up.edu.ph; cltiburan@up.edu.ph
[2]Laboratory of Regional Planning, Graduate School of Global Environmental Studies, Kyoto University, Japan
- saizen.izuru.4n@kyoto-u.ac.jp

Keywords: Geomorphology, Otsu Thresholding, Canny-Edge Detection, Sinuosity Index Analysis, Water Index, Landsat

Abstract

This study focused on quantifying changes in river morphology using a remote sensing approach. Historical river planforms were derived from Landsat images processed through Google Earth Engine platform. Five water indices were used: the MBWI, NDWI, MNDWI, AWEIshadow and AWEInoshadow. To automatically extract surface image, combined OTSU-thresholding and Edge-Detection Approached was employed. The analysis covered the years 1990 to 2023 at 5-year interval. Baseline river planform was established using a 1970 topographic map from NAMRIA. For the sinuosity analysis, the entire stretch of Pagsanjan River was divided into 10 1-kilometer segments, starting from the first river junction of the main river to the outlet. Results show that the most significant change is observed near the outlet between the baseline year 1970 and 1990. An eastward shift was also observed during this year. Aside from these observed changes, no substantial changes in sinuosity or channel migrations were detected from 1990 onward. This stability can be attributed to the implementation of riverbank stabilization in the early 1990s. These findings demonstrate the effectiveness of remote sensing in morphological analysis and emphasize the long-term importance of river stabilization measures in maintaining channel. This is particularly important in a country, such as the Philippines, which is frequently visited by Typhoon which often lead to increase in channel discharge and subsequent changes in channel planforms.

1. Introduction

A watershed is a land area drained by a stream or fixed body of water and its tributaries having a common outlet for surface run-off. Over the years and through the improvement of different management strategies for environmental protection and management, a watershed-based approach has proven to be very effective. In essence, it dwells in the idea that elements of the watershed are connected, and understanding the events on the upstream can help explain the events on the downstream.

In the Philippines, most research and projects apply the watershed approach, wherein the extent of a watershed is the primary unit of investigation or analysis. Corresponding analyses such as river water quality and quantity, which are deemed as major indicators of watershed health, are being pursued and conducted to further understand the dynamics happening in the landscape. These analyses are often included in developing integrated watershed management plans. Unfortunately, very few efforts are conducted to understand river morphology, even though, previous research projects have already defined the importance of channel morphology in understanding river behavior, and subsequently, watershed behavior. Majority of research in the Philippines focus on watershed characterization using different geomorphological parameters to understand the physical characteristics of a watershed (Boothroyd, et al., 2023, Cruz et al., 2012). While research focusing on morphological changes and its implications to river management are very limited, as similarly stated in the recent paper of Tolentino et al. (2022). Currently, only a number of morphological studies are available related to river morphology such as the work of Boothroyd et al. (2025) on geomorphic river mobility, Naputo et al. (2023) on morphological evolution of Binahaan River in Palo, Leyte, and the decadal river analysis of Dingle et al. (2019). With this, this study aims to contribute in the limited literature in river morphology study in the Philippines by looking into the planform morphology of the Pagsanjan River in Laguna, Philippines using remote sensing approach, how it changes over time, and its potential impacts to river management.

2. Methodology

The selected area for the study is the main channel of the Pagsanjan-Lumban Watershed (PLW). The location map of Pagsanjan-Lumban watershed is presented in Figure 1. It is in the southeastern part of Laguna Lake and covers 6 municipalities of Laguna namely: Cavinti, Kalayaan, Lumban, Majayjay, Magdalena, and Pagsanjan. It has 4 major subwatersheds: Balanac, Bombongan, Caliraya, and Lewin; and two man-made lakes: Caliraya and Lumot Lakes. It has a total land area of 45,445 ha, is the second-largest watershed draining in Laguna Lake, and has the highest contribution of water to the lake (Cruz et al. 2012).

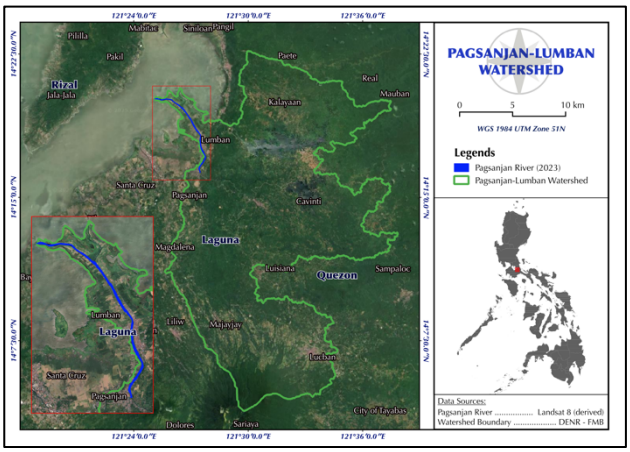

Figure 1. Location map of Pagsanjan-Lumban Watershed

This contribution has been peer-reviewed. The double-blind peer-review was conducted on the basis of the full paper.
https://doi.org/10.5194/isprs-annals-X-5-W4-2025-75-2026 | © Author(s) 2026. CC BY 4.0 License.

The PLW drains its water through the Pagsanjan River. The river stretches approximately 9.9km from its furthest junction in Barangay Poblacion I and Magdapio in the municipality of Pagsanjan as measured in GIS. The outlet is covered by the Barangay Wawa from the municipality of Lumban, Laguna.

2.1 Data Sources

2.1.1 Topographic Maps: Topographic maps produced by the National Mapping and Resource Information Authority (NAMRIA) will be used to generate the baseline river channel of PLW. These maps are scaled at 1:50,000 and based on NAMRIA website these were originally published by the US Army Service from 1947 to 1953 aerial photographs.

The baseline river channel extent was digitized from 1:50000 NAMRIA topographic maps as presented in Figure 2. Map name Paete, map sheet number 7271-I with corresponding PNTMS sheet 3229-I. The channel was digitized from bank to bank extending from the outlet to the first main junction near San Pedro, Pagsanjan, Laguna.

Figure 2. Portion of map sheet 7271-I Paete showing the portion of Pagsanjan River.

2.1.2 Landsat Satellite Images: Annual river channel extent was extracted from Landsat satellite images starting 1988. It was initially planned to analyze from the start of Landsat legacy. However, Landsat 1 has a different spatial resolution of 60m which was opted not to include. To minimize the effect of seasonality in the image, the image composite for each year was created using the image collection from March 1 to May 31 of each year.

2.2 Surface Water Detection and Extraction

All image processing was implemented in Google Earth Engine (GEE), an open-source platform for planetary analysis (Gorelick et al. 2017). A multi-temporal cloud masking technique was applied to remove clouds and cloud shadow in the image, then the median reduction was used to generate a single image composite from the image collection of each year. This allowed the selection of median values from an image collection on a per-pixel basis creating a cloud-free image composite.

Automatic extraction of water from the different spectral indices was done by determining the threshold value that separates the water pixel from non-water pixels. For this study, the Otsu thresholding technique was employed (Otsu, 1979). Otsu thresholding divides the image gray value by class maximizing variance. This provided a single value that optimally separates water from non-water pixels in the image extent. To complement this and identify the threshold locally focused on Pagsanjan River, the Otsu algorithm was coupled with Canny-Edge detection which can improve feature extraction by filtering out weak and noisy edges (Mapurisa and Sithole, 2022; Ali and Clausi, 2001).

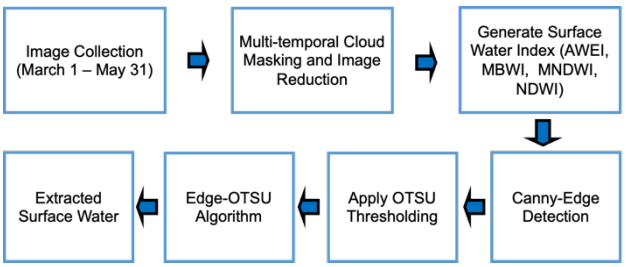

Figure 3. Methodological framework for automatic surface water extraction.

2.2.1 Identification of best spectral indices for surface water extraction: The following water indices were used in the study and the best-performing index will be used to extract annual river channel extent for the planform morphology analysis.

2.2.1.1 Normalized Difference Water Index (NDWI): NDWI by McFeeters (1996) is one of the first water indices developed. It is designed to remove the presence of soil and vegetation in the image to extract surface water features.

$$NDWI = \frac{(Green - NIR)}{(Green + NIR)} \quad (1)$$

where: NIR = Near infrared band

2.2.1.2 Modified Normalized Difference Water Index (MNDWI): Xu (2006) proposed a modification from NDWI, the MNDWI to address the issue of NDWI in extracting water features in urban environment.

$$MNDWI = \frac{(Green - SWIR1)}{(Green + SWIR1)} \quad (2)$$

where: SWIR = Shortwave infrared band

2.2.1.3 Multi-band Water Index (MBWI): MBWI is a water index developed by Wang et al. (2018) utilizing multiple spectral bands to maximize the difference between water surface and non-water surface. It can be computed using the equation below:

$$NBWI = 2 * Green - Red - NIR - SWIR1 - SWIR2 \quad (3)$$

2.2.1.4 Automatic Water Extraction Index (AWEI): Feyisa et al. (2018) developed AWEI to improve the classification of water against areas with dark surfaces. This index has two variations for different applications. AWEIshadow is designed to enhance the water classification against shadow pixels. On the other hand, AWEInoshadow is best applied in areas where the effect of shadow is not prominent.

$$AWEI_{shadow} = Blue + 2.5 * Green - 1.5(NIR + SWIR) - 0.25 * SWIR2 \quad (4)$$

$$AWEI_{no\ shadow} = 4 * (Green - NIR) - ((0.25 * NIR) + (2.75 * SWIR1)) \quad (5)$$

The results were then validated using a manually digitized extent from the same Landsat Image cross validated with high resolution Google Earth image. For the accuracy assessment, only the overall accuracy (OA) and Kappa Coefficient of 200 randomly generated points per focused area were used since this is just a binary classification of where a pixel is water or non-water. Additionally, a comparison of the extracted area was assessed.

2.2.2 Annual River Extraction: After the assessment of different surface water indices, the best-performing index was used to extract the river extent to be used for planform analysis. An annual composite created from a collection of Landsat images from March 1 to May 31 of each year was produced. The initial date filter was extended per month until December of each year for the years where clouds are still present especially along the stretch of Pagsanjan River. The specific Landsat mission used for each year is indicated in Table 1.

Landsat Image	Year of Analysis
Landsat 4	1988 - 1995
Landsat 5	1996 - 2013
Landsat 8	2014 - 2023

Table 1. Landsat product used per analysis year.

Automatic annual river extraction was implemented in GEE following the same methodology in Figure 3 but only using the best-performing water index identified.

2.2.3 Sinuosity Index (SI) Analysis: Channel patterns can be analyzed by measuring the amount of its curvature and threading, or its sinuosity. The Sinuosity Index (SI) is defined as the ratio of the straight line of the channel to the length along the meandering channel Mittal et al. (2023). The index can be used to determine which part of the channel has significant changes in position over time. SI can be computed using the equation below:

$$SI = Channel\ Length/Valley\ Length \quad (6)$$

In this study, the stretch of the Pagsanjan River was divided into 10 sections and the SI for each section was computed using the RiverMetrics plugin in QGIS (De Rosa et al. 2017). This plugin allows the computation of sinuosity from a river centerline.

3. Results and Discussion

3.1 Surface Water Detection

The study assessed 5 different water indices: AWEI (shadow and no shadow), MBWI, NDWI and MNDWI to determine which index will be used in extracting annual riverbanks for morphological analysis. Four focused areas were identified to determine the performance of each index, namely: (1) Sta. Cruz River, Pagsanjan River, Pagsanjan outlet and Lumot Lake. These four focused areas have different characteristics, the Sta. Cruz River outlet is a characterized with high built-up areas in both banks which, the Pagsanjan River is somewhat similar with Sta. Cruz River outlet but has a combination of built-up areas and vegetation along the banks, Pagsanjan outlet covers both the outlet of the river characterized with agricultural areas with less built-up and a portion of the Laguna Lake, lastly, the Lumot Lake which focuses only on the extent of the lake and its immediate environment. The four focused areas were selected due to the different characteristics which is a good test on the performance of the different water index.

The extracted water extents are illustrated in Figure 4. Visually, the difference in the output is not very noticeable, but a significant difference on the extent of the MNDWI is very noticeable especially in the Lumot Lake. As shown in Table 2, MNDWI recorded the lowest area for Lumot lake with 338.13ha while the highest water extent was from AWEIshadow. In addition, it is also important to note the detected water pixels in both variations of AWEI which are outside the extent of analysis. This indicates the sensitivity of AWEI especially in areas with shadow (Feyisa et al., 2018). Although these can be identified as misclassified pixels if the area of analysis considered is the whole image extent, but since the study is only interested in detecting water extent in Pagsanjan River, it is not relevant in the study. Moreover, the identified local canny-otsu threshold used to separate the water from non-water pixels was focused on the Pagsanjan River area only and not the entire image.

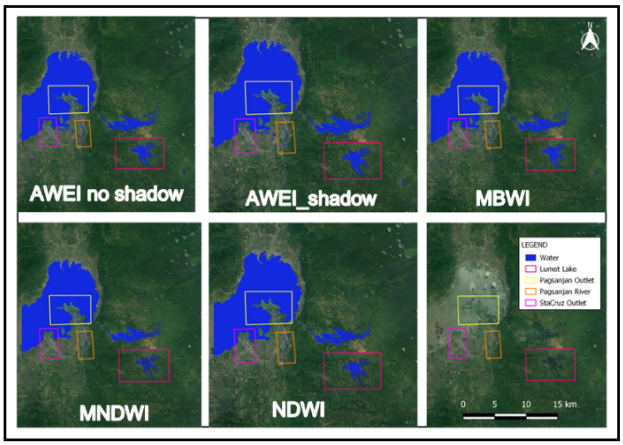

Figure 4. Detected and extracted surface water for each focus area using different surface water index.

Table 2 presents the area extent of extracted water for each index. For this analysis, the absolute value of residual is considered as the assessment measure of whether an index perform better that the others. As indicated in the previous section, there was an obvious difference in the extent of detected water pixels in Lumot lake in MNDW compared to other indices. As indicated in the Table 2, the MNDWI extracted water extent of 288.36 ha and a residual value of 265.11 ha when compared to the digitized value of 553.47 ha. For Lumot Lake, AWEshadow performed has the lowest residual value of -46.074 ha. Similarly, AWEshadow has the lowest residual in Pagsanjan River. This may indicate the flexibility of this index in detecting water pixels in image with different background pixels.

The output of accuracy assessment is indicated in Table 3. As previously stated, since this is a binary classification, only the OA and Kappa coefficient were used in assessing the performance of each band. As observed NDWI performed better in areas where there is not much presence of built-up areas such as Pagsanjan and worse in areas with built-up areas such as Pagsanjan River and Sta. Cruz outlet which is similar to other studies (Masocha et al. 2018; Sarp and Ozcelick, 2017). This is one of the distinguishing features of NDWI and one of the reasons for developing the MNDWI (Xu, 2006). MNDWI did not perform well in terms of OA and Kappa for all focused areas, it is the second-best performing index in Pagsanjan outlet and the got the lowest OA for other focused areas. As for MBWI and

AWEInoshadow, they performed well on all focused areas in terms of OA, Kappa and areas of extracted water pixels.

Focus Area	True Area (ha)	AWEI no Shadow		AWEI shadow		MBWI		MNDWI		NDWI	
		Area (ha)	Residual	Area (ha)	Residual	Area (ha)	Residual	Area (ha)	Residual	Area (ha)	Residual
Pagsanjan Outlet	2198.5	2313.8	-115.3	2301.2	-102.7	2301.9	-103.4	2277.26	-78.8	2227.1	-28.6
Pagsanjan River	42.3	38.1	4.2	42.6	-0.3	38.8	3.5	25.8	16.5	23.2	19.1
Sta Cruz Outlet	329.0	337.2	-8.2	348.3	-19.2	337.1	-8.1	319.4	9.6	311.1	17.9
Lumot Lake	553.5	498.6	54.9	507.5	46.1	502.8	50.7	288.4	265.1	338.1	215.3

Table 2. Extent and area analysis of detected surface water pixel using different water index. *(Note: index with the lowest absolute value of residual was considered as the most accurate and performed best in water detection and extraction.)*

On the other hand, AWEIshadow performed best in two of the four focused areas, in both Pagsanjan River and Sta. Cruz River outlet with presence of vegetation and urban areas. This define the flexibility of AWEIshadow for surface water detection and can be considered as the best performing index for Pagsanjan River annual surface water detection and extraction. The performance of AWEIshadow can be attributed to its main feature as it performed well in areas with shadows, especially the effects of topography (Yang et al. 2015), and areas that are constantly affected by clouds and cloud shadows. Feyisa et al. (2018) developed this index as an improvement of other existing water indices and has produced better accuracy under various environmental conditions compared to other spectral indices. Although, same with the output of Yang et al. (2015), AWEI may not be the best index to use in coastal areas and tidal flats.

Focus Area	AWEI no shadow		AWEI shadow		MBWI		MNDWI		NDWI	
	OA (%)	Kappa (%)	OA (%)	Kappa (%)	OA (%)	Kappa (%)	OA (%)	Kappa (%)	OA (%)	Kappa (%)
Pagsanjan Outlet	93.0	85.9	93.0	85.9	93.0	85.9	93.5	86.0	95.0	86.5
Pagsanjan River	97.0	73.5	99.0	75.4	97.5	73.9	96.0	72.4	94.0	69.8
Sta Cruz Outlet	97.0	87.5	97.0	87.7	97.0	87.60	95.5	87.3	96.5	87.3
Lumot Lake	98.7	86.7	98.5	85.8	98.5	85.8	89.5	83.6	93.5	84.6

Table 3. Accuracy Assessment results of different surface water indices in four focus areas.

3.2 Annual River Extraction

The annual surface water of Pagsanjan River was derived using the best-performing index, the AWEIshadow but the analysis focused on a 5-year interval as illustrated in Figure 5. Each of the extracted surface water is overlaid with the baseline riverbanks from the NAMRIA map.

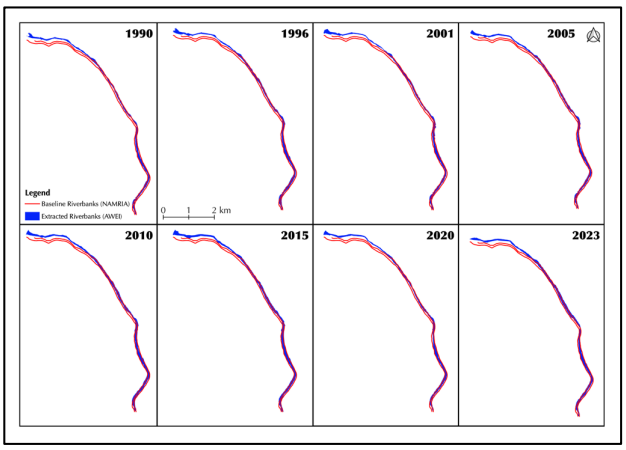

Figure 5. Baseline riverbank and extracted annual river extent using AWEI.

The upstream most portion of the river shows a negligible difference between the baseline river and the extracted river for all the analysis years. On the other hand, an observable difference is present in the outlet of the river where it shifted eastward from the baseline river. No obvious differences were observed when all extracted surface water extent were compared with each other aside from the river edges due that can be attributed to the resolution of Landsat image of 30m.

The lack of observable shifting of riverbanks or changes in river shape due to the presence of riverbank stabilization walls of Pagsanjan River, as shown in Figure 6. The river cross sectional survey in Figure 7 shows that the whole stretch of Pagsanjan River has a riverbank stabilization wall towering up to 10 meters for both banks which prevented the degradation of riverbank from its construction. This is one of the main reasons how the Pagsanjan River maintained its planform morphology and no significant changes occurred for the last 30 years.

Figure 6. Photos of Pagsanjan River as viewed from Lumban Bridge. The retaining walls stretches from the upstream of Balanac Bridge and Cavinti bridge until the river outlet.

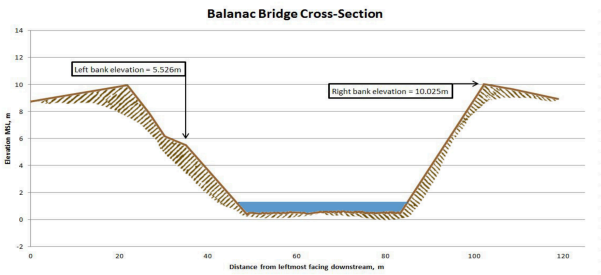

Figure 7. River cross-section indicating the height of retaining walls in Pagsanjan River. (Note: Taken from the report of Phil-LiDAR 1 UPLB, Paringit and Abucay, 2017).

However, it is important to note that sedimentation is still prevalent (Hernandez et al. 2012), mainly due to the agricultural activities in upstream portion of the area. Evidently, there are observable differences in the outlet of the river as observed by visually interpreting the annual satellite images also shown the formation of delta.

3.3 Sinuosity Analysis

The baseline river centerline was digitized from NAMRIA map, while centerlines of other years were automatically generated from the riverbanks of each extracted surface water using the HCMGIS plugin in QGIS (Quach, 2018). This plugin allows user to create centerline from polygons. Other morphological assessment used thalweg in assessing river sinuosity, however, since there were no records of that, the derived centerlines were used. To gain insight on the profile of Pagsanjan River, an extracted image from the report of Paringit and Abucay (2017) is shown in Figure 8.

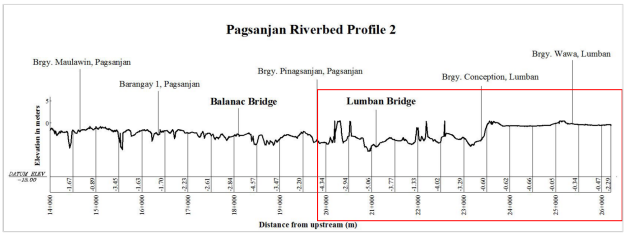

Figure 8. River profile of Pagsanjan River. (Note: Taken from the report of Phil-LiDAR 1 UPLB (Paringit and Abucay, 2017). The red box is the same as the analysis extent in this study).

The survey was conducted around 2016 during the Phil-LiDAR project, hence, there may be differences in the present profile of the river. But as shown on the profile (Figure 8), the elevation of Pagsanjan River bed ranges from -5 to 5m above sea level and is almost level for the most part of the river, this is an indication that the sediments from the upstream are being distributed equally in the river and the higher elevation close to the mouth of the river indicates the deposition of the sediments (Edmonds and Slingerland, 2007), which eventually lead to delta formation. Deposition along the banks where not shown in the report but it was assumed to be uniform for the whole stretch of the Pagsanjan River due to the presence of retaining walls.

The baseline centerline and derived annual centerlines from satellite images are plotted in Figure 9. The river was divided into 9 stations labels as S-1 to S-9 representing various distances from the upstream to the mouth of the river. This was done to easily identify where changes in planform morphology occurred.

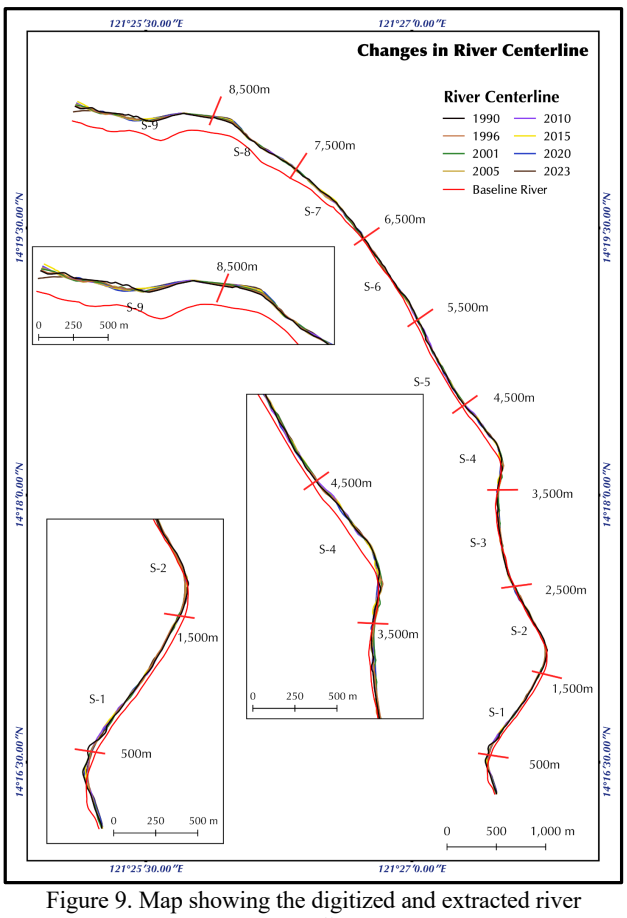

Figure 9. Map showing the digitized and extracted river centerline.

Like what was observed in the derived river channel, the only noticeable differences were when the individual index-derived centerline was compared with the baseline centerline, most especially in the river outlet where the centerline shifted eastward. When measured, the shift was around 197m eastward for all analysis years, and this is considered as the highest shift in centerline value for all the river section. Another observable shift is in S-1 with an average westward shift of 40m. In S-4, a shift of 60m from the 3,500m point from upstream is observed and narrowed to 30m as it passes through the 4,500m part of the river.

The observed shifting in the upstream section of Pagsanjan River may be negligible when compared to the shift near the outlet. These observed shifting may only be due to the innate errors in georeferencing the NAMRIA basemap and inconsistency in digitizing as similarly observed in other related studies (Mittal et al. 2023; Rowland et al. 2016). However, the relatively large shift in the downstream portion of the river indicates its vulnerability to morphological changes and had the riverbank retaining walls not done, it would have resulted to massive changes in the river.

The Sinuosity Index (SI) for each centerline, baseline and index-derived, was calculated automatically using the RiverMetrics plugin. As mentioned, the Pagsanjan River was divided into 9 segments to better understand the morphological changes in river. The detail for each segment is indicated in Table 4 with the sinuosity values for each segment and the graph in Figure 10 was presented to illustrate the trend for each station per analysis year.

SI is just one of the many important indices in understanding river morphology. Generally, it has an inverse relationship with riverbank erosion (Nath and Gosh 2022), hence an increase in river erosion will result to lower value of SI, which means that the river is somewhat straight or not meandering. In this study, the river reach is classified as straight, sinuous or meandering following the classification of Brice (1964) where in river reach with SI $\geq$ 1.5 is considered as meandering, SI $\leq$ 1.1 is straight, and reach with 1.1 $\leq$ SI $\geq$ 1.5 is considered as sinuous reach. Following this reach classification, all the river reaches of Pagsanjan River is classified as straight. The highest SI recorded is in S1 with 1.1114, roughly in the sinuous category.

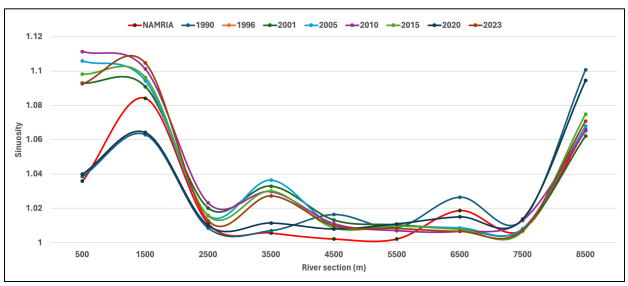

Figure 10. Sinuosity Index graph of the Pagsanjan River segments.

Changes in SI for each reach from the baseline would indicate morphological changes such as riverbank erosion, formation of oxbow lake if present and other changes. For the Pagsanjan River, there is a minimal up to negligible changes observed in river reaches from the baseline river up to the present date. High and most changes in SI occurred from the baseline river SI to the 1990 SI, afterwards, minimal changes in SI values are observed which can already be attributed as the effect of automatic extract of surface water using remote sensing and not really from the morphological changes in the river. Relating this observation to the observed migration of river centerline observed near the outlet, it can be concluded that the changes in river migration may be due to errors when the original base map was created as well as the innate errors in georeferencing.

Station	Length (km)	Baseline	1990	1996	2001	2005	2010	2015	2020	2023
S-1	0-1.5	1.036	1.039	1.036	1.093	1.106	1.111	1.098	1.040	1.093
S-2	1.5-2.5	1.084	1.063	1.084	1.091	1.094	1.101	1.096	1.064	1.105
S-3	2.5-3.5	1.011	1.009	1.011	1.020	1.016	1.023	1.016	1.010	1.013
S-4	3.5-4.5	1.006	1.007	1.006	1.033	1.036	1.030	1.030	1.011	1.027
S-5	4.5-5.5	1.002	1.016	1.002	1.013	1.010	1.011	1.009	1.008	1.010
S-6	5.5-6.5	1.002	1.009	1.002	1.010	1.010	1.007	1.010	1.011	1.008
S-7	6.5-7.5	1.019	1.027	1.019	1.008	1.009	1.007	1.008	1.015	1.007
S-8	7.5-8.5	1.008	1.013	1.008	1.008	1.008	1.013	1.007	1.014	1.007
S-9	5.6-9.9	1.066	1.101	1.066	1.062	1.068	1.065	1.075	1.095	1.071
Average		**1.026**	**1.031**	**1.031**	**1.038**	**1.040**	**1.041**	**1.039**	**1.030**	**1.038**

Table 4. Sinuosity Index of Pagsanjan River reaches from 1990 to 2023.

Based on the overall results of the study, there is not significant changes in morphological characteristics of Pagsanjan River that occurred since the 1990s. This is mainly due to the presence of riverbank stabilization, specifically, retaining walls in the whole stretch of Pagsanjan River. Although, the records regarding the construction of this retaining walls were not provided, it is already observable in the satellite images starting 1988. For Pagsanjan, the construction of retaining walls preserved the riverbanks and prevented degradation and potentially negative changes in river planform over time. In addition, flooding due to overflowing of water has been greatly reduced over time and most of the flooding incidences in the area are due to basin effect in the nearby areas mainly due to improper drainage.

4. Conclusion

The present study focused on assessing planform morphological assessment of Pagsanjan River, the main channel of Pagsanjan-Lumban Watershed. The study, first, compared and assessed five of the most used surface water indices namely: AWEI (shadow and no shadow), MBWI, NDWI and MNDWI. Based on the initial assessment, AWEIshadow performed-best in terms of overall accuracy and Kappa Coefficient. AWEI outperformed the other water index mainly due to its flexibility in separating water pixels in complex environment and especially in areas affected with shadows due to presence of mountains and cloud shadows. The annual river extent was the derived using AWEIshadow and

automatically extracted based on the threshold derived from the combination of Otsu and Canny-Edge detection.

The annual river extent was used to generate the riverbanks and centerline and compared to the baseline riverbanks and centerline from NAMRIA topographic maps. River shifting and centerline migration results indicated a negligible value which are attributed to the innate error in georeferencing and inconsistencies in digitizing. The results were further supported by the values derived from Sinuosity Index analysis indicating minimal changes in sinuosity in river reaches of Pagsanjan River, which is mainly due to the presence of riverbank stabilization measures in the river which prevented drastic changes in river morphology.

Although the study was initially interested in determining how the dynamics of river morphology in Pagsanjan, the results indicated the importance and benefits of riverbank stabilization in controlling river parameters. Not only that they can prevent floods due to overflowing of river, but they also prevented the drastic changes in river channel over time.

While the study produced significant and meaningful results, it is still greatly limited by the resolution of the images used, since only Landsat has the available free dataset to do long term change analysis, such as this study. Nevertheless, it is interesting to implement similar studies in other rivers in the Philippines, especially those with a complex morphology and with other activities like quarrying. Another, interesting aspects that should be done is determining the relationship of land cover changes of the watershed and its morphology, as well as the sedimentation rates and delta formation.

Acknowledgement

The authors would like to thank the financial support provided by Kyoto University Graduate School of Global Environmental Science Seed Research Funding Program.

References

Ali, M., Clausi, D., 2001. Using the Canny edge detector for feature extraction and enhancement of remote sensing images. *Proc. Scanning Present Resolving Future IEEE Int. Geosci. Remote Sens. Symp.,* pp. 2298-2300, Jul. 2001. doi.org/10.1109/IGARSS.2001.977981

Boothroyd, R.J., Williams, R.D., Hoey, T.B., Brierly, G.J., Tolentino, P.L.M., Guardian, E.L., Reyes, J.C.M.O., Sabillo, C.J., Quick, L., Perez, J.E.G., David, C.P., 2025. Big data show idiosyncratic patterns and rates of geomorphic river mobility. *Nature Communications* 16, 3263. doi.org/10.1038/s41467-025-58427-9

Boothroyd, R.J., Williams, R.D., Hoey, T.B., MacDonell, C., Tolentino, P.L.M, Quick, L., Guardian, E.L., Reyes, C.M., Sabillo, C.J., Perez, G.J.E., David, C.P., 2023. National-scale geodatabase of catchment characteristics in the Philippines for river management applications. *PLOS One*, 18 (3), e0281933. doi.org/10.1371/journal.pone.0281933

Brice, J.C., 1964. *Channel Patterns and Terraces of the Loup Rivers in Nebraska.* United States Government Printing Office, Washington, pp. 1-40.

Cruz, R.V.O., Pillas, M., Castillo, H.C., Hernandez, E.C., 2012. Pagsanjan-Lumban catchment, Philippines: Summary of biophysical characteristics of the catchment, background to site selection and instrumentation. *Agricultural Water Management,* 106 (2012) 3-7

De Rosa, P., Cencetti, C., Fredduzzi, A., 2017. An automated method for river sinuosity calculation using QGIS. *GEAM Geoingegneria Ambientale e Mineraria,*151 (2), 81-84.

Dingle, E.H., Paringit, E.C., Tolentino, P.L., Williams, R.D., Hoey, T.B., Barrett, B., Long, H., Smiley, C., Stott, E., 2019. Decadal-scale morphological adjustment of a lowland tropical river. *Geomorphology*, *333*, 30-42. doi.org/10.1016/j.geomorph.2019.01.022

Edmonds, D.A. and Slingerland, R.L., 2007. Mechanics of river mouth bar formation: Implications for the morphodynamics of delta distributary networks. *J. Geophys. Res.-Earth Surf.* 112. doi.org/10.1029/2006JF000574

Feyisa, G.L., Meilby, H., Fensholt, R., Proud, S.R., 2014. Automated water extraction index: A new technique for surface water mapping using Landsat imagery. *Remote Sensing of Env.* 140, 23–35. doi.org/10.1016/j.rse.2013.08.029

Gorelick, N., Hancher, M., Dixon, M., Ilyushchenko, S., Thau, D., Moore, R., 2017. Google Earth Engine: Planetary-scale geospatial analysis for everyone. *Remote Sensing of Environment* 202, 18-27. doi.org/10.1016/j.rse.2017.06.031

Hernandez, E.C., Henderson, A., Oliver, D.P., 2012. Effects of changing land use in the Pagsanjan–Lumban catchment on suspended sediment loads to Laguna de Bay, Philippines. *Agricultural Water Management* 106, pp. 8-16. doi.org/10.1016/j.agwat.2011.08.012

Mapurisa, W., Sithole, G., 2022. Improved Edge Detection for Satellite Images. *ISPRS Annals of Photogrammetry, Remote Sensing and Spatial Information Sciences* 52, pp. 185–192. doi.org/10.5194/isprs-annals-V-2-2022-185-2022.

McFeeters, S.K., 1996. The use of the Normalized Difference Water Index (NDWI) in the delineation of open water features. *International Journal of Remote Sensing*, 17 (7):1425–32. doi.org/10.1080/01431169608948714

Masocha, M., Dubeb, T., Makorea, M., Shekedea, M.D., Funani, J., 2018. Surface water bodies mapping in Zimbabwe using landsat 8 OLI multispectral imagery: A comparison of multiple water indices. *Physics and Chemistry of the Earth* 106, 63-67. doi.org/10.1016/j.pce.2018.05.005

Mittal, R., Said, S., Beg, M., 2022. Assessment of Changes in Planform Morphology of the Upper Yamuna River Segment, India, Using Remote Sensing and GIS. *Physical Geography* 44:4, 446-477. doi.org/10.1080/02723646.2022.2090656

Nath, A., Gosh, S., 2022. The influence of urbanization on the morphology of the Barak River floodplain in Cachar District, Assam. *Water Policy,* 24 (12): 1876–1894. doi.org/10.2166/wp.2022.133

Naputo, K.M., Distrajo, R.B., Ortiz, K.M., Gutierrez, N.A., 2023. Morphological Evolution of the Binahaan River, Palo, Leyte, 6501, Philippines. *Aquatic Sciences and Engineering*, 38 (3), 160-167. doi.org/10.26650/ASE20231244025

Otsu, N., 1979. A Threshold Selection Method from Gray-Level Histograms. *IEEE Transactions on Systems, Man, and Cybernetics* 9, (1) 62-66. doi.org/10.1109/TSMC.1979.4310076

Paringit, E.C., Abucay, E.R., 2017. LiDAR Surveys and Flood Mapping Report of Pagsanjan River, in Enrico C. Paringit, (Ed.), Flood Hazard Mapping of the Philippines using LIDAR, Quezon City: University of the Philippines Training Center on Geodesy and Photogrammetry-254pp.

Quach, T., 2018. HCMGIS plugin for QGIS. https://plugins.qgis.org/plugins/HCMGIS/#plugin-about

Rowland, J.C., Shelef, E., Pope, P.A., Muss, J., Gangodagamage, C., Brumby, S.P., Wilson, C.J., 2016. A morphology independent methodology for quantifying planview river change and characteristics from remotely sensed imagery. *Remote Sensing of Environment,* 184, 212–228. doi.org/10.1016/j.rse.2016.07.005

Sarp, G., Ozcelik, M., 2017. Water body extraction and change detection using time series: A case study of Lake Burdur, Turkey. *Journal of Taibah University for Science* 11, 381–391. dx.doi.org/10.1016/j.jtusci.2016.04.005

Tolentino, P. L.M., Perez, J. E., Guardian, E. L., Boothroyd, R. J., Hoey, T. B., Williams, R. D., Fryirs, K. A., Brierley, G. J., David, C. P., 2022. River Styles and stream power analysis reveal the diversity of fluvial morphology in a Philippine tropical catchment. *Geoscience Letters*, *9* (1), 1-18. doi.org/10.1186/s40562-022-00211-4

Wang, X., Xie, S., Zhang, X., Chen, C., Guo, H., Du, J., Duan, Z., 2018. A Multi-Band Water Index (MBWI) for automated extraction of surface water from Landsat 8 OLI Imagery. *Int. J. Appl. Earth Obs Geoinformation* 68, 73-91. doi.org/10.1016/j.jag.2018.01.018

Yang, Y., Liu, Y., Zhou, M., Zhang, S., Zhan, W., Sun, C., Duan, Y., 2015. Landsat 8 OLI image based terrestrial water extraction from heterogeneous backgrounds using a re!ectance homogenization approach. *Remote Sensing of Environment* 171, 14–32. dx.doi.org/10.1016/j.rse.2015.10.005

Xu, H., 2006. Modification of normalised difference water index (NDWI) to enhance open water features in remotely sensed imagery. *Int. J. Remote Sensing,* 27, 3025–3033. doi.org/10.1080/01431160600589179